



RESEARCH ARTICLE

Drawn out of the shadows: Surveying secretive forest species with camera trap distance sampling

Mattia Bessone^{1,2}  | Hjalmar S. Kühl^{3,4} | Gottfried Hohmann³ | Ilka Herbing⁵ | Kouame Paul N'Goran⁶ | Papy Asanzi² | Pedro B. Da Costa² | Violette Dérozier² | Ernest D. B. Fotsing² | Bernard Ikembelo Beka² | Mpongo D. Iyomi² | Iyomi B. Iyatshi⁷ | Pierre Kafando⁸ | Mbangi A. Kambere² | Dissondet B. Moundzoho² | Musubaho L. K. Wanzalire² | Barbara Fruth^{1,2,9} 

¹School of Biological and Environmental Sciences, Liverpool John Moores University, Liverpool, UK; ²Faculty of Biology/Department of Neurobiology, Ludwig Maximilians University of Munich, Planegg-Martinsried, Germany; ³Department of Primatology, Max Planck Institute for Evolutionary Anthropology, Leipzig, Germany; ⁴German Centre for Integrative Biodiversity Research (iDiv) Halle-Leipzig-Jena, Leipzig, Germany; ⁵Department of Africa and South America, WWF Germany, Berlin, Germany; ⁶WWF Regional Office for Africa—Yaoundé Hub, Yaoundé, Cameroon; ⁷Institut Congolais pour la Conservation de la Nature (ICCN), Kinshasa, Democratic Republic of the Congo; ⁸WWF in the Democratic Republic of the Congo, Kinshasa, Democratic Republic of the Congo and ⁹Centre for Research and Conservation, Royal Zoological Society of Antwerp, Antwerp, Belgium

Correspondence

Mattia Bessone

Email: M.Bessone@2018.ljmu.ac.uk

Funding information

Kreditanstalt für Wiederaufbau (KfW Group) on behalf of the German Government and WWF Germany; Liverpool John Moores University

Handling Editor: Fernanda Michalski

Abstract

1. With animal species disappearing at unprecedented rates, we need an efficient monitoring method providing reliable estimates of population density and abundance, critical for the assessment of population status and trend.
2. We deployed 160 camera traps (CTs) systematically over 743 locations covering 17,127 km² of evergreen lowland rainforest of Salonga National Park, block South, Democratic Republic of the Congo. We evaluated the applicability of CT distance sampling (CTDS) to species different in size and behaviour. To improve precision of estimates, we evaluated two methods estimating species' availability ('A') for detection by CTs.
3. We recorded 16,700 video clips, revealing 43 different animal taxa. We estimated densities of 14 species differing in physical, behavioural and ecological traits, and extracted species-specific availability from available video footage using two methods (a) 'ACa' (Cappelle et al. [2019] *Am. J. Primatol.*, 81, e22962) and (b) 'ARo' (Rowcliffe et al. [2014] *Methods Ecol. Evol.* 5, 1170). With sample sizes being large enough, we found minor differences between ACa and ARo in estimated densities. In contrast, low detectability and reactivity to the camera were main sources of bias. CTDS proved efficient for estimating density of homogeneously rather than patchily distributed species.
4. *Synthesis and applications.* Our application of camera trap distance sampling (CTDS) to a diverse vertebrate community demonstrates the enormous potential of this

This is an open access article under the terms of the Creative Commons Attribution-NonCommercial-NoDerivs License, which permits use and distribution in any medium, provided the original work is properly cited, the use is non-commercial and no modifications or adaptations are made.

© 2020 The Authors. *Journal of Applied Ecology* published by John Wiley & Sons Ltd on behalf of British Ecological Society

methodology for surveys of terrestrial wildlife, allowing rapid assessments of species' status and trends that can translate into effective conservation strategies. By providing the first estimates of understudied species such as the Congo peafowl, the giant ground pangolin and the cusimanses, CTDS may be used as a tool to revise these species' conservation status in the IUCN Red List of Threatened Species. Based on the constraints we encountered, we identify improvements to the current application, enhancing the general applicability of this method.

KEYWORDS

biomonitoring, camera trap, cryptic species, density estimation, distance sampling, multi-species, Salonga National Park, unmarked population

1 | INTRODUCTION

The use of camera traps (CTs) to study wildlife has seen an exponential increase in the last decade (Burton et al., 2015), offering innovative approaches for obtaining species' distribution, density, abundance, behaviour and community structure in an economical and minimally invasive way (Rovero & Zimmermann, 2016). Animal density is an extremely informative parameter in community ecology, providing data for monitoring temporal trends in population status and comparing populations across sites (Nichols & Williams, 2006), crucial information for effective wildlife conservation.

The first density estimators based on CT footage were designed for large, individually recognizable species, using a capture–recapture (CR) framework (Karanth & Nichols, 1998). The method was applied to few mammals, mainly felids identified by their coat pattern (Jackson, Roe, Wangchuk, & Hunter, 2006; Karanth, 1995). However, defining the effective surveyed area was problematic and CR methods estimated population size within an area of unknown size, rather than density (Sollmann, Mohamed, & Kelly, 2013). *Mark-reSight* methods (MS; Rich et al., 2014) and spatially explicit capture–recapture methods (SECR; Efford, Borchers, & Byrom, 2009) were a big improvement. By estimating the area effectively sampled, density estimates became statistically valid (Sollmann, Linkie, Haidir, & Macdonald, 2014). However, requiring at least a proportion of individuals to be recognizable, they were not applicable to all species. Recently, the development of statistical estimators of animal density has overcome these limitations. SECR methods have been extended allowing density estimates of unmarked populations (Chandler & Royle, 2013). Here, sampling effort must be spatially intensive and estimates lack precision unless supplemented with auxiliary data such as genetic sampling or telemetry (Evans & Rittenhouse, 2018; Linden, Sirén, & Pekins, 2018; Sollmann et al., 2014). Random encounter models (REMs; Rowcliffe, Field, Turvey, & Carbone, 2008) were considered a promising development. REMs assumed a certain detection within an estimated area in front of the camera and, by using the gas model of Hutchinson and Waser (2007) to describe animal movement, required estimates of average animal speed for estimating animal density. Animal speed however, is hard

to estimate accurately, and REMs broad applicability is still being tested (Chauvenet, Gill, Smith, Ward, & Massei, 2017; Sollmann et al., 2013). To address these issues, recent studies have used a modified version of REMs. Nakashima, Fukasawa, and Samejima (2017) replaced animal speed with the time animals remained in the camera field of view (obtained from recorded videos), whereas Campos-Candela, Palmer, Balle, and Alós (2017) in a simulation study and Moeller, Lukacs, and Horne (2018) in a study on elks *Cervus canadensis*, circumvented the need for animal average speed by collapsing sampling occasions into predetermined instantaneous moments where the surface covered by the camera field of view was known and 100% detectability assumed. Although these methods were a promising development for estimating density of unmarked species, they remain to be tested in various field situations and, as some (e.g. Campos Candela et al., 2018; Nakashima et al., 2017) are mathematically demanding, broad applicability without a user-friendly software seems unlikely.

Camera trap distance sampling (CTDS; Howe, Buckland, Després-Einspenner, & Kühl, 2017) is another recently proposed method for density estimations of unmarked populations. It uses a distance sampling (DS) approach (Buckland et al., 2001), adjusting point transect DS to the use of CTs. Similar to Moeller et al. (2017) and Campos-Candela et al. (2017), CTDS makes use of predetermined instantaneous snapshot moments, but assumes 100% detection at 0 m only, accounting for imperfect detection by modelling detectability as a function of distance. In addition, CTs only detect animals when available, a problem when studying arboreal or subterranean species. Therefore, CTDS requires estimates of species-specific availability 'A', that is, the proportion of time a species is available for detection. So far, two methods have been used for estimating 'A': (a) 'ACa' (Cappelle, Després-Einspenner, Howe, Boesch, & Kühl, 2019) refers to the time of activity 'T_i' with T_i being defined as the number of 1-hr intervals with at least one video; (b) 'ARo' (Rowcliffe, Kays, Kranstauber, Carbone, & Jansen, 2014) estimates 'A' by fitting a circular kernel distributions to times of independent detections, with the peak of activity defined by the maximum value of the kernel distribution. Importantly, in both methods 'A' is extracted from the same videos used for estimating density. CTDS was applied to

wild populations of Maxwell's duiker *Philantomba maxwellii* (Howe et al., 2017), and Western chimpanzees *Pan troglodytes verus* in Taï National Park, Côte d'Ivoire (Cappelle et al., 2019) returning unbiased estimates for the latter. In addition, by using a DS approach, CTDS takes advantage of a consolidated mathematical framework, open-source software and a vast community of users and developers, making the method easily accessible. Therefore, CTDS could be considered among the most promising methods to assess animal density, particularly suitable for habitats where species taking advantage of dense vegetation for their cryptic existence are rarely encountered.

Our planet's tropical rainforests, particularly the Amazonian and the Congo basins, provide these features. Disappearing with unprecedented speed, ecological information for the vast majority of terrestrial vertebrates is urgently required (IUCN, 2019). Central Africa's Congo basin provides 1,620,000 km² of evergreen rainforests, with 1,000 bird and 400 mammal species currently known (Campbell, 2005). Its heart, the *Cuvette Centrale*, 800,000 km² in size situated south of the Congo River, Democratic Republic of the Congo (DRC), has the continent's largest protected area of pristine African lowland rainforest: Salonga National Park (SNP), an IUCN

World Heritage Site. Here, we estimate vertebrate density by applying CTDS to the large and remote South block of Salonga National Park, assessing applicability of the methodology in relation to species-specific properties such as (a) size; (b) activity patterns; (c) sociality; (d) abundance; (e) distribution and (f) reactivity to CTs. The latter referring to any responsive behaviour occurring because of the presence of an observer (i.e. the CTs) causing the animal to modify its travelling trajectory. This either by (a) moving away from the camera (avoidance), (b) approaching it (attraction), or (c) stopping, standing in front of the camera.

2 | MATERIALS AND METHODS

2.1 | Study area

Salonga National Park (36,000 km²), situated in the *Cuvette Centrale*, DRC (Figure 1a), consists of two blocks, North and South. We investigated block South (17,127 km²), composed of 99% of primary lowland mixed forest, 1% of savannahs, regenerating forest, cultivation, marshes and water bodies (Bessone et al., 2019).

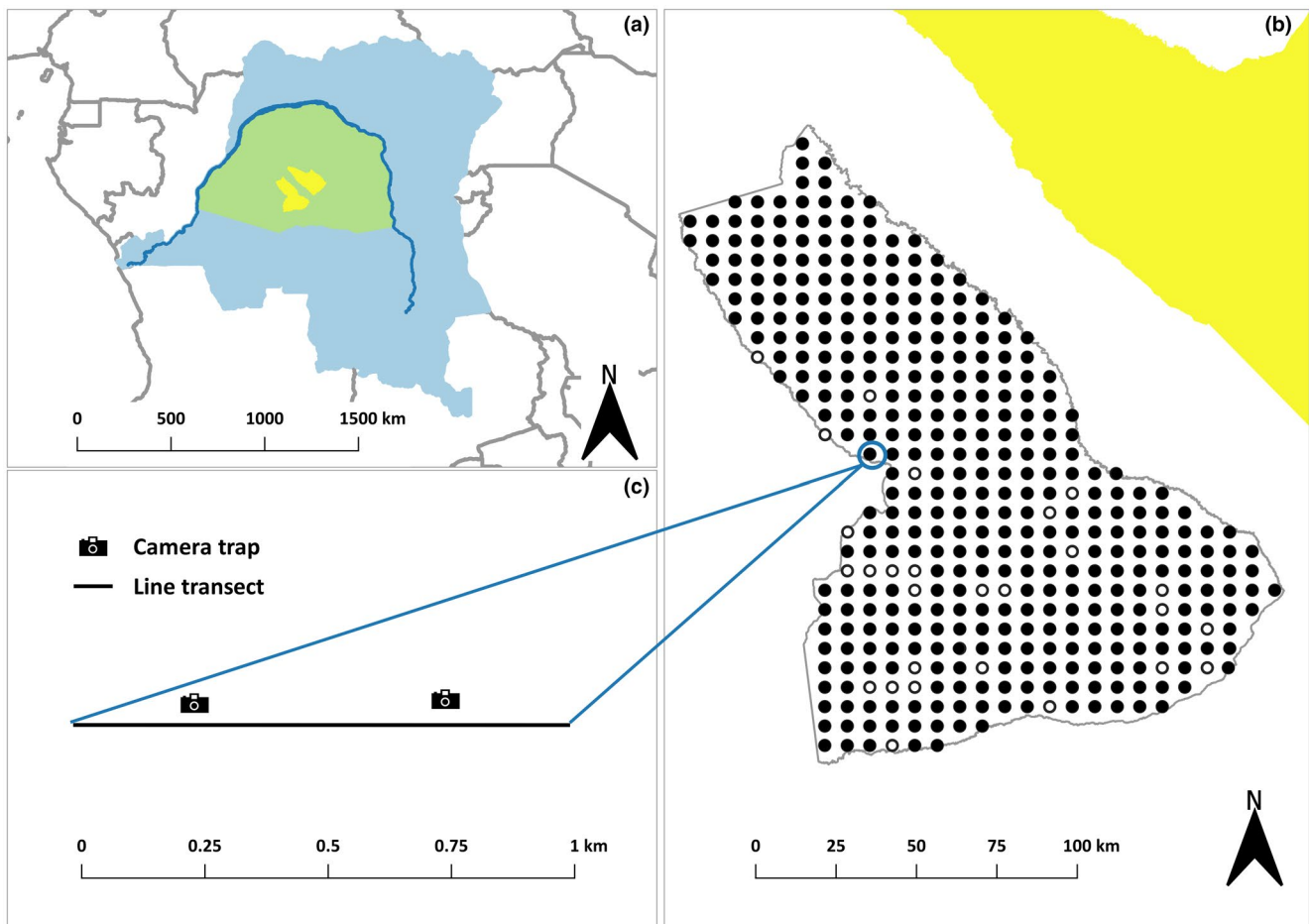


FIGURE 1 Location and survey design: (a) Democratic Republic of the Congo (DRC; light blue) with Congo river (blue line), *Cuvette Centrale* (green) and Salonga National Park (SNP; yellow); (b) SNP, block South with surveyed (black dots) and unsurveyed (white dots) line transects; (c) Camera trap locations along line transect

2.2 | Data collection

Camera trap data were collected between September 2016 and May 2018 as part of a comprehensive biodiversity inventory (PNS-Survey©), conducted along 405 systematically placed sample units (i.e. line transects), generated from a random origin. The 1 km transects running east–west were evenly spaced by 6 km (Figure 1b). Two infrared CTs (Bushnell Trophy CamTM, Model 119776), with angle of view $\theta = 45^\circ$ and inter-trigger lag time = 1 s, were set up at 250 and 750 m from the beginning of each transect (Figure 1c). To avoid disturbance caused by the passage of field teams, cameras were systematically positioned 50 m to the north or south of the transect line, oriented north between 70 and 90 cm above-ground. Given the size of SNP and the limited number of devices ($n = 160$), the study area was divided into 37 sub-areas covering 380 km² on average (range = 72–1,188 km², $SD = 274.8$), each surveyed once. CTs were relocated to a new sub-area after a minimum of 2 weeks (average = 38.4 days, range 14–78, $SD = 12.4$).

Of the 405 transects, 27 were not surveyed due to their proximity to major rivers, or armed poachers, resulting into 378 surveyed line transects (Figure 1b). Due to logistical constraints, one transect remained without, and four transects with only one CT each, resulting in 750 sampling locations. Time of installation, habitat type and GPS location were noted for each device. Cameras were active 24 hr/day and sensor sensitivity was set to 'high'. For a discussion of potential limitations of our survey design, see Appendix S1.

2.3 | Camera trap distance sampling

2.3.1 | Measurements

Following Howe et al. (2017), we measured distances between the CT's lens (i.e. 0 m) and the midpoint of each detected animal (=radial distances) in each video at predetermined snapshot moments (=observations) by comparing animal locations to 1 m distance labels recorded during camera installation (from 1 to 12 m). Predetermined snapshot moments represent observations at specific times of day, starting with a snapshot at midnight 00 hr 00 min 00 s with an interval between snapshots 't' set to 2 s, a value considered appropriate to obtain adequate sample sizes even for fast moving and rare species (Howe et al., 2017). Temporal effort is then determined by the value of t (the longer 't', the lower the effort—see Appendix S2).

We expected that species-specific features could potentially affect CTDS estimates. Therefore, for each observation, we also recorded (a) individual maturity (immature/adult), (b) animal group size and (c) reactive behaviours (see Appendix S3).

2.3.2 | Species-specific availability

We corrected for species-specific availability 'A' applying (a) 'ACa' (Cappelle et al., 2019) and (b) 'ARo' (Rowcliffe et al., 2014), calculating

ARo by using the R package 'activity' (R Core Team, 2019; see Figure S1). In order to ensure independence of observations of times of detection, we used the number of capture events, defined as the first video recording the same individual/animal group, while subsequent videos of the same individual/group were discarded. A new event was recorded when a different individual/animal group entered the field of view.

2.3.3 | Density estimation

Densities were estimated by applying the formula of Howe et al. (2017; see Appendix S2 for further details). All operational days, excluding days of camera installation and retrieval, were considered when calculating survey effort.

As reactivity to CTs is expected to induce bias (Buckland et al., 2001), we discarded all observations where animal behaviour indicated a reaction to CTs. Then, we left- and/or right-truncated each dataset after visual inspection of the histogram of observed radial distances (see Figure S2). We fitted the detection functions to the remaining radial distances and calculated species-specific density in distance 7.3 (Thomas et al., 2010), correcting for both ACa and ARo, and considering six CTDS models (half normal with 0 and 1 hermite polynomial adjustment terms; hazard rate with 0 and 1 cosine adjustments terms; uniform with 1 and 2 cosine adjustment terms).

In CTDS, violation of the assumption of independence of observations is expected. Violation does not affect point estimates of abundance (Buckland et al., 2001), but introduces 'over-dispersion', which is partially addressed by defining predetermined instantaneous snapshot moments (Howe et al., 2017; Moeller et al., 2017). In addition, the assumption can be relaxed by estimating variances using a nonparametric bootstrap, resampling points with replacement (Buckland et al., 2001), and by using model selection methods adjusted for over-dispersed data. Accordingly, we estimated variance from 999 bootstrap resamples, with replacement across camera locations, and selected between competing models comparing QAIC scores, following a two-step method (Howe, Buckland, Després-Einspenner, & Kühl, 2019).

2.4 | Considered species

Recorded species were considered suitable for density estimation if (a) the number of independent capture events was ≥ 20 ; (b) the number of recorded radial distances was ≥ 80 (Buckland, Rexstad, Marques, & Oedekoven, 2015). To test general applicability of the method, we selected species showing differences in size, activity, abundance and distribution patterns. Information on the following species-specific traits was acquired from published literature: (a) body mass, a proxy of body size (Smith et al., 2003); (b) activity pattern (diurnal, nocturnal or crepuscular); (c) sociality (gregarious or solitary); (d) expected abundance; (e) expected distribution

(homogeneous or heterogeneous) (2–5: Kingdon et al., 2013) and (f) conservation status (IUCN Red List of Endangered Species, 2019).

3 | RESULTS

A total of 160 CTs were fully functional and active at 743 locations. Total effort was 27,045 camera days, returning 16,734 videos showing animals belonging to 43 different taxa (see Table S1). Average species richness per location was 4.7 (range 0–24, $SD = 3.04$). Of these 43 taxa, 29 provided adequate data for density estimation. Table 1 shows 14 out of these, selected due to their differences in biological (body mass), behavioural (activity pattern, sociality),

ecological (abundance, distribution) and conservation (IUCN status) traits. Except for the endemic Congo peafowl, all chosen species were mammals.

Table 2 shows species-specific information obtained from CTs, including activity times, availability according to Cappelle et al. (2019) and Rowcliffe et al. (2014; examples provided in Figure 2), as well as truncation distance. Detectability positively correlated with body size, with small-sized species being undetected within the first 2 m from the camera (Figure 3).

Of the 14 species, immature individuals were never detected in seven, made up less than 10% of observations in another four, and more than 10% in three species only (Table 2). Therefore, we decided to exclude observations of immature individuals, providing population estimates for adults only. Three different types

TABLE 1 Species (Common name, *scientific name*) selected for method evaluation. Body mass (average in kg; Smith et al., 2003); Activity pattern (sD = strictly diurnal; sN = strictly nocturnal; mD = mainly diurnal; mN = mainly nocturnal; Cr = crepuscular); Sociality (G = gregarious; S = solitary); Approximate expected abundance (n/km^2) available from literature; Distribution available from literature; IUCN status (IUCN, 2019). Reference: Kingdon et al. (2013)

ID	Species	Body mass (kg)	Activity pattern	Sociality	Approximate expected abundance [n/km^2]	Distribution	IUCN status
1	Congo peafowl ^a <i>Afropavo congensis</i>	1.4	sD	G	Unknown	Homogeneous	VU
2	Forest elephant <i>Loxodonta cyclotis</i>	3,940.0	mD	G	0.05	Heterogeneous	EN
3	Bonobo <i>Pan paniscus</i>	34.0	sD	G	0.42	Homogeneous	EN
4	Allen's swamp monkey <i>Allenopithecus nigroviridis</i>	4.7	sD	G	100	Heterogeneous	LC
5	Honey badger <i>Mellivora capensis</i>	8.0	mD	S	0.03	Homogeneous	LC
6	African golden cat <i>Caracal aurata</i>	10.6	mD	S	0.04–0.1 ^b	Homogeneous	VU
7	Genets <i>Genetta</i> sp.	2.0–1.9 ^c	sN	S	0.8–4.5 ^c	Homogeneous	LC
8	Cusimanses <i>Crossarchus</i> sp.	0.7–1.5 ^d	mD	G	Unknown	Homogeneous	LC
9	Aardvark <i>Orycteropus afer</i>	52.3	sN	S	1–2	Homogeneous	LC
10	Giant ground pangolin <i>Smutsia gigantea</i>	33.0	sN	S	Unknown	Unknown	VU
11	Sitatunga <i>Tragelaphus spekii</i>	78.0	mD	S	92–180	Heterogeneous	LC
12	Water chevrotain <i>Hyemoschus aquaticus</i>	10.8	sN	S	1.5–5	Homogeneous	LC
13	Brush-tailed porcupine <i>Atherurus africanus</i>	1.9	sN	S	2.4–13	Homogeneous	LC
14	Four-toed sengi <i>Petrodromus tetradactylus</i>	0.2	Cr	S	210	Homogeneous	LC

^aMcGowan, Kirwan, & Sharpe (2019).

^bBahaa-el-din et al. (2016).

^c*Genetta servalina* and *G. maculata*.

^d*Crossarchus alexandri* and *C. ansorgei*.

TABLE 2 Species-specific information obtained from camera traps (CTs). Individual locations: Number of CT locations with detections >0; Capture events: Number of video-clips; Total Radial distances: Total of measured radial distances; Radial distances 'Immatures' (%): Number of radial distances of immature individuals (percentage of total); Radial distances 'Reactivity' (%): Number of radial distances of reactive individuals (percentage of total); Activity time T_1 [hours]: number of activity hours per 24-hr-day used when calculating specific availability after Cappelle et al. (2019); Availability (ACa): specific availability calculated after Cappelle et al. (2019); Availability (ARo) (SE): specific availability (standard error) calculated over 24 hr after Rowcliffe et al. (2014); Truncation [m] left; right: meter(s) of left and right-truncation of radial distances

ID	Species	Individual locations	Capture events	Total Radial distances	Radial distances 'Immatures' (%)	Radial distances 'Reactivity' (%)	Activity time T_1 [hours] ^a	Availability (ACa) ^a	Availability (ARo) (SE) ^a	Truncation [m] left; right
1	Congo peafowl	73	137	3,104	249 (8%)	240 (8%)	12	0.57	0.34 (0.04)	1; 8
2	Forest elephant	14	20	840	68 (8%)	676 (80%)	24	0.15	0.34 (0.10)	0; 12
3	Bonobo	66	100	5,604	1,376 (25%)	515 (11%)	14	0.45	0.34 (0.05)	0; 12
4	Allen's swamp monkey	12	49	1,067	81 (17%)	209 (19%)	12	0.31	0.39 (0.04)	3; 8
5	Honey badger	18	21	217	None	48 (22%)	11	0.38	0.28 (0.07)	0; 7
6	African golden cat	23	25	84	None	6 (7%)	13	0.34	0.45 (0.07)	0; 7
7	Genets	63	95	431	None	None	11	0.61	0.43 (0.03)	2; 7
8	Cusimanses	24	34	1,301	72 (5%)	None	13	0.44	0.44 (0.06)	2; 7
9	Aardvark	46	54	354	None	25 (7%)	12	0.45	0.31 (0.04)	0; 6
10	Giant ground pangolin	15	24	119	None	None	11	0.50	0.40 (0.07)	1; 8
11	Sitatunga	10	23	417	101 (24%)	None	14	0.41	0.64 (0.11)	0; 7
12	Water chevrotain	38	152	1,462	None	None	12	0.61	0.34 (0.03)	1; 6
13	Brush-tailed porcupine	140	527	1,765	48 (3%)	None	12	0.62	0.34 (0.02)	2; 8
14	Four-toed sengi	7	40	216	None	None	13	0.31	0.28 (0.05)	2; 5

^aSee Appendix S2.

FIGURE 2 Camera trap-derived daily activity patterns for (a) Capture events < 50 (Elephant); (b) Capture events > 50 (Aardvark); (c) Capture events > 100 (Water chevrotain). Solid lines show availability (ACa) as relative frequency of capture events for each hour interval according to Cappelle et al. (2019); Dashed blue lines show availability (ARo) as relative frequency of capture events fitted over 24 hr according to Rowcliffe et al. (2014)

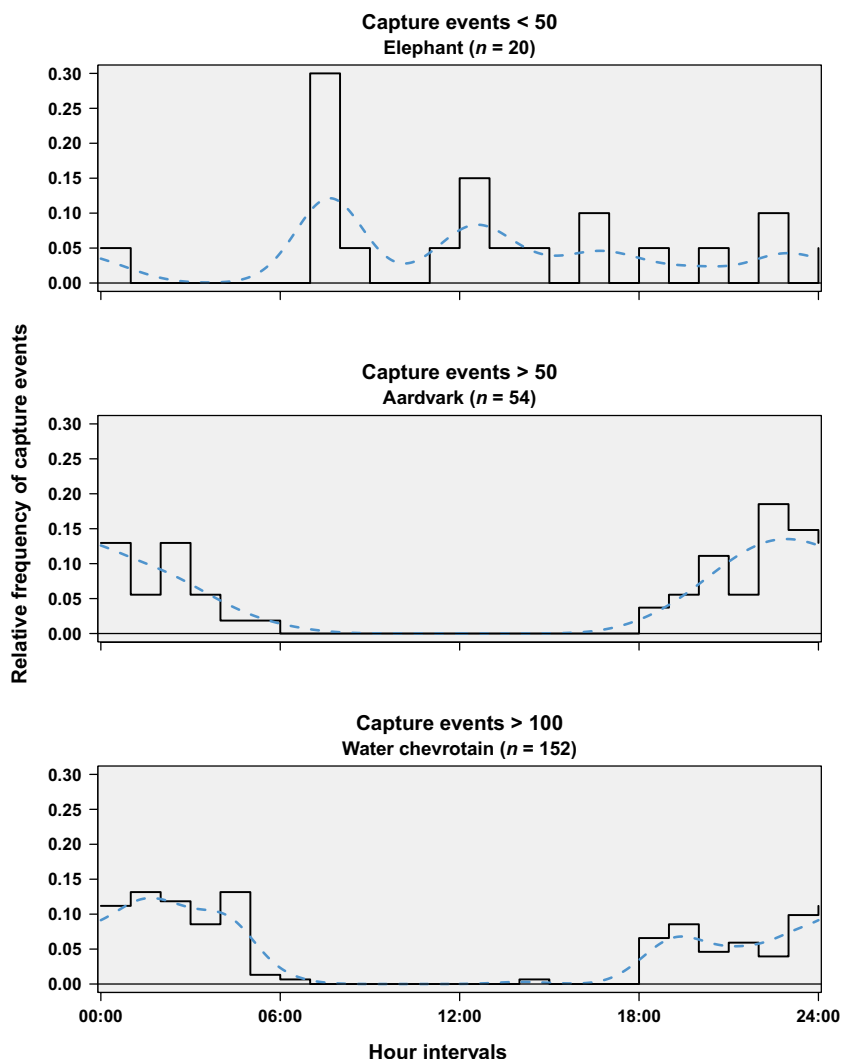
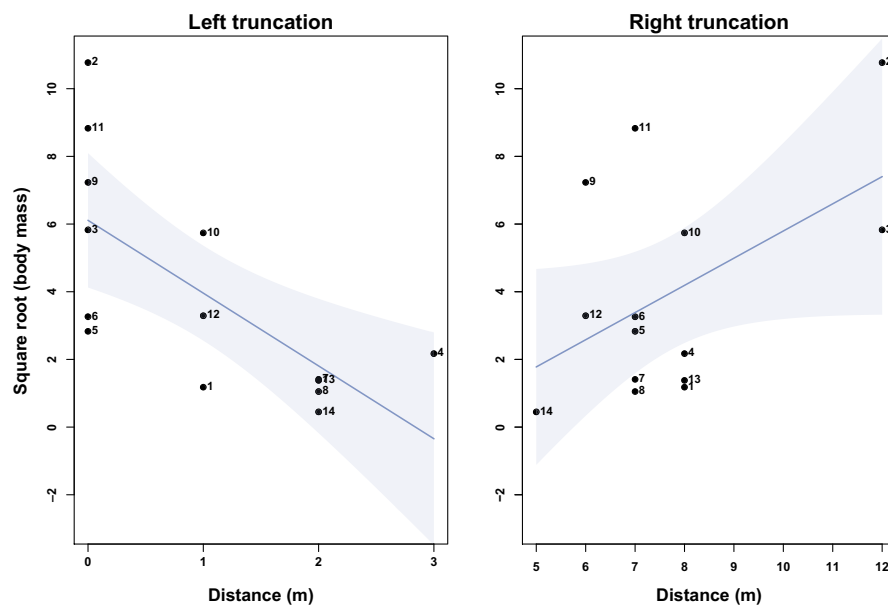


FIGURE 3 Species-specific truncation distances (m) for Left-truncation (left); and Right-truncation (right). Blue lines represent linear regression (left-truncation $R^2 = 0.48$, $p < 0.01$; right-truncation $R^2 = 0.19$, $p = 0.07$) with 95% confidence intervals (light blue areas). Black dot with number indicates species; numbers see 'ID' in Table 1



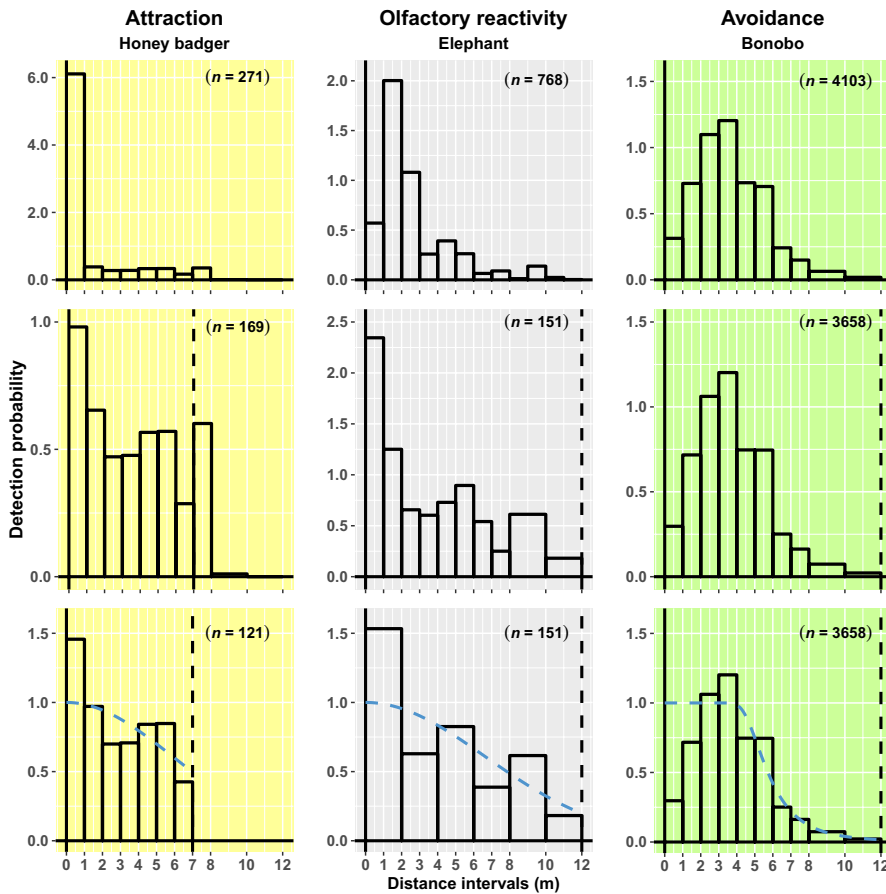
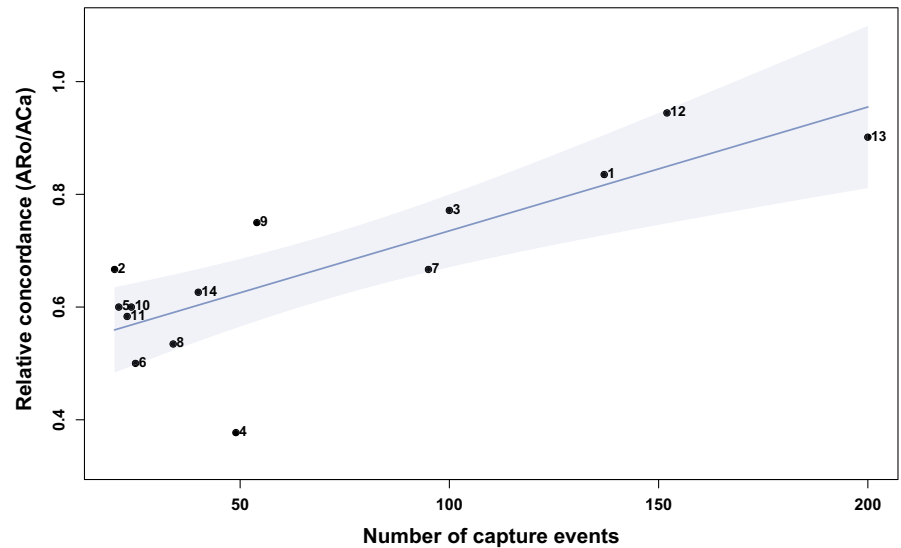


FIGURE 4 Reactivity to camera traps. Columns: Left (yellow): Attraction (honey badger); Middle (grey): Olfactory (elephant); Right (green): Avoidance (bonobo). Rows: Top: reactive observations included; Middle: reactive observation excluded; Bottom: final fitted model after right-truncation (honey badger); binning (elephant); as is (bonobo). Bars provide detection probability as function of distances (1.0 = 100%) prior to truncation (reactivity observations included). Dashed black lines show distances of truncation. Dashed blue lines detection probability as a function of distance (reactivity observations discarded)

TABLE 3 Species-specific density estimates. Selected model for density estimation showing (a) key function (HN = Half normal; HR = Hazard rate; UNI = Uniform); (b) series expansion (*co* = cosine; *hp* = hermite polynomial); (c) adjustment terms; Radial distances (=observations): Number of measurements after truncation and discarding of immatures and reactive individuals; Density (*ACa*) [ind/km²] (95% CIs): Density of mature individuals per km² (in bold) corrected for availability using *ACa* (Cappelle et al., 2019) with 95% confidence intervals (CIs); Density (*ARo*) [ind/km²] (95% CIs): Density of mature individuals per km² (in bold) corrected for availability using *ARo* (Rowcliffe et al., 2014) with 95% confidence intervals (CIs); C.V. *ACa*; *ARo*: Estimated coefficient of variation for (a) Density (*ACa*), (b) Density (*ARo*)

ID	Species	Selected model a; b; c	Radial distances	Density (<i>ACa</i>) [ind/km ²] (95% CIs)	Density (<i>ARo</i>) [ind/km ²] (95% CIs)	C.V. <i>ACa</i> ; <i>ARo</i>
1	Congo peafowl	UNI; <i>co</i> ; 1	2,383	0.91 (0.66–1.27)	0.76 (0.55–1.06)	0.17; 0.17
2	Forest elephant	HN; <i>hp</i> ; 0	151	0.03 (0.01–0.07)	0.02 (0.01–0.03)	0.44; 0.45
3	Bonobo	HR; <i>co</i> ; 0	3,658	0.70 (0.32–1.53)	0.54 (0.24–1.21)	0.41; 0.43
4	Allen's swamp monkey	HN; <i>hp</i> ; 0	691	0.53 (0.24–1.14)	0.20 (0.09–0.43)	0.41; 0.40
5	Honey badger	HN; <i>hp</i> ; 0	121	0.05 (0.02–0.09)	0.03 (0.01–0.06)	0.39; 0.41
6	African golden cat	HN; <i>hp</i> ; 0	78	0.04 (0.02–0.07)	0.02 (0.01–0.03)	0.36; 0.36
7	Genets	HN; <i>hp</i> ; 0	374	0.27 (0.17–0.43)	0.18 (0.11–0.28)	0.24; 0.23
8	Cusimanses	HN; <i>hp</i> ; 0	1,104	1.16 (0.58–2.36)	0.62 (0.31–1.26)	0.37; 0.37
9	Aardvark	HN; <i>hp</i> ; 0	255	0.20 (0.10–0.34)	0.15 (0.09–0.26)	0.27; 0.28
10	Giant ground pangolin	HN; <i>hp</i> ; 0	112	0.05 (0.02–0.13)	0.03 (0.01–0.08)	0.50; 0.54
11	Sitatunga	HN; <i>hp</i> ; 0	253	0.12 (0.03–0.42)	0.07 (0.02–0.25)	0.71; 0.74
12	Water chevrotain	HN; <i>hp</i> ; 0	1,250	0.72 (0.38–1.35)	0.68 (0.37–1.27)	0.33; 0.32
13	Brush-tailed porcupine	HN; <i>hp</i> ; 0	1,624	0.71 (0.48–1.03)	0.64 (0.44–0.96)	0.20; 0.20
14	Four-toed sengi	HR; <i>co</i> ; 0	191	289.46 (2.67–31,294.00)	181.09 (2.16–15,177.00)	17.20; 12.71

FIGURE 5 Relative species-specific concordance of density estimates corrected with ARo (Rowcliffe et al., 2014) and ACa (Cappelle et al., 2019) by number of capture events. Relative concordance (ARo/ACa): 1.0 = 100% concordance. Blue line represents linear regression ($R^2 = 0.62$, $p < 0.01$) with 95% confidence intervals (light blue area). Black dot with number indicates species; numbers see 'ID' in Table 1



of reaction to CTs (i.e. attraction, avoidance and olfactory) were recognized in seven species (Table 2); examples are provided in Figure 4.

Table 3 shows density estimates for each species after bootstrapping, corrected for species-specific activity patterns, providing selected model and coefficient of variation. ACa-corrected estimates consistently provided higher densities than ARo, with ACa-corrected and ARo-corrected estimates being similar with at least 100 capture events (Table 2 and Figure 5). Estimates' precision significantly improved with a higher number of individual locations with at least one capture event (log-transformed— $R^2 = 0.63$; $p < 0.01$). A similar trend, with precision increasing with higher numbers of recorded radial distances or estimated densities, was not significant (see Figure S3). These results were confirmed by a multiple regression analysis, where precision was modelled as a function of the three aforementioned variables (see Table S2), suggesting precision was mainly driven by the number of individual locations and sample size.

4 | DISCUSSION

Our results are the first application of CTDS to a multi-species animal community and show the enormous potential of this method for biomonitoring. However, as in other CTs studies (Burton et al., 2015), biological, ecological and behavioural features affected specific detectability. In the following, we will discuss how six of these features could influence the applicability of CTDS: (a) body size/mass; (b) sociality; (c) activity pattern; (d) distribution; (e) abundance and (f) reactivity to the camera.

4.1 | Body size/mass

Our results confirm previous studies (Rowcliffe, Carbone, Jansen, Kays, & Kranstauber, 2011; Sollmann et al., 2013; Tobler, Carrillo-Percastegui, Pitman, Mares, & Powell, 2008), showing that body-size

positively correlates with detectability (Table 2; Figure 3). In such cases, we left-truncated our data when estimating density, a method known to effectively address low detectability at short distances (Buckland et al., 2001). However, left-truncation implies loss of data needed for achieving accurate estimates, especially for rare species. Therefore, we suggest that deploying cameras at a height of 50 cm above-ground would increase detection rates of small-sized species. Although surprisingly found to be detected imperfectly within the first 2 m from the CT despite an average shoulder height of 95 cm (Figure 4), left-truncation was not applied to the bonobo, for reasons explained later ('6. Reactivity to camera'). As expected, elephants were detected at short distances. However, given their size, both body length and width were considered when measuring radial distances, and fit was improved by binning data in 2-m intervals (Figure 4).

4.2 | Sociality

When applying DS to gregarious species, detection rates may be inflated, as detecting the first animal in a group increases the probability of detecting others (Treves, Mwima, Plumtre, & Isoke, 2010). However, we found no clear evidence for overestimated density in gregarious species (see Table S3) and obtained satisfactory coefficients of variation (<25%) for both brush-tailed porcupine (solitary) and Congo peafowl (gregarious), with low precision equally affecting solitary and gregarious species when capture events were rare (Table 3).

4.3 | Activity patterns

Although differences in the specific availability calculated according to Cappelle et al. (2019), and Rowcliffe et al. (2014) were minor with large sample sizes, ARo presented major advantages: (a) calculations provided standard errors of estimated availabilities (that

could be included in the estimation of total variance of density) and (b) values appeared to be less influenced by the peak of observation and stochasticity (Figure 2; Table 3). Both methods rely on the assumption that at peak time, 100% of the population is available for detection (Rowcliffe et al., 2014), with asynchronous activity patterns of individuals within species leading to an over-estimation of activity time, hence underestimated densities. *ARo* is consistently calculated over 24 hr, whereas *ACa* refers to the hour intervals of observed activity, considering activity hours with one capture event only (Figure 2). In *ACa*, activity intervals may remain undetected due to low sample size, potentially causing underestimation of survey effort. For example, we observed elephants from 20 capture events only, revealing activity in 11 of 24-hr intervals (Figure 2). Elephant activity however, is reported to occur throughout a 24-hr-day (Kely et al., 2019), suggesting we missed part of the species' activity time. While available knowledge could be used to interpret results according to species-specific ecology and behaviour, with *ARo* activity time fitted over 24 hr, additional sources of variation were avoided (Figure 2). In sum, sample sizes larger than 100 capture events allowed accurate and consistent estimates (Figure 5). Limited numbers of capture events however lead to underestimated *ACa*, inflating density values (Tables 2 and 3). Therefore, we recommend longer CT deployment, allowing a minimum of 100 capture events per species and the use *ARo* (Rowcliffe et al., 2014) for the calculation of specific availability. Unless supported by large enough sample sizes, comparing specific availability and density estimates across different studies is precarious and should be performed with care.

4.4 | Distribution

We expected high variability in encounter rates for heterogeneously distributed species, leading to imprecise density estimates due to spatial variation (Buckland et al., 2001). In fact, all the species we expected being heterogeneously distributed (Table 1), showed a coefficient of variation >40%, due to low sample size and observations obtained from very few locations (Table 3—but see also Figure S3). Future research should aim at increased spatial effort with synchronous camera deployment to reduce potential bias and strengthen precision (Buckland et al., 2015). When this is not possible, a stratified random design might increase estimate precision (Foster & Harmsen, 2012).

4.5 | Abundance

Consequently, while precision was more satisfactory for abundant species, it was also good (C.V. below 35%) for rare, but widespread species such as the genets and the armadillo (Table 3—but see Figure S3), with precision being mainly a function of sample size (i.e. number of radial distances) and heterogeneous distribution (i.e. number of individual locations with at least one capture event—see Table S2). When estimating density of abundant species, a limiting factor was

the time required for distance measurements from video-clips. To reduce time of analysis, (a) snapshot interval t could be increased, or (b) observations may be restricted to peak of activity only (Howe et al., 2017). For validation, we compared the full with the reduced methods for all species, and obtained consistent densities despite increased snapshot intervals and peak of activity observations only (see Table S4). However, in the case of rarer species, the application of these methods would further reduce the number of exploitable radial distances, making safe estimates impossible.

4.6 | Reactivity to the camera

Reactivity to the camera is known to bias density estimates, as it violates the assumptions of DS (Buckland et al., 2001). Attraction to CTs, providing a high number of observations close to the camera has been previously addressed with left-truncation (Cappelle et al., 2019). However, to minimize induced bias, we consistently excluded all snapshots showing evident reactivity to the camera from analysis, not only for species attracted to CTs, such as the honey badger (Figure 4), but also for the elephants, showing strong olfactory reactivity by insistently smelling the area in front of the camera (regardless of the distance interval). In elephants, when using all observations including the 80% showing reactivity, estimates were inflated up to two orders of magnitude (Figure 4). Avoidance is less frequent, but Kalan et al. (2019) reported it for the bonobo. We confirm bonobos' avoidance of the camera, resulting in fewer observations within the first 2 m (Figure 5). However, bonobos were not undetected, but rather observed further away, and left-truncation was not applicable. Lack of detection close to the camera can be levelled out by excess of detection further away (Buckland et al., 2015), but densities were inflated by 15% because bonobo neophobia seems to be coupled with curiosity from a secure distance. Therefore, we discarded all snapshots showing reactive behaviours. This study suggests reactivity to CTs being the most impacting form of bias in CTDS. Not accounting for reactivity could result in largely inflated density estimates, and future studies should carefully examine the videos to detect reactive behaviours. To reduce visual and olfactory reactivity, we recommend to either deploy CTs for at least 1 month prior to the survey, allowing animals to habituate to cameras; or record reference distance labels after the survey, reducing the time of CT set-up, and by that 'contamination' with human odour. If neither is possible, methods not influenced by reactivity to CTs (e.g. SECR), is to be favoured over CTDS.

5 | CONCLUSIONS

Camera trap distance sampling is an excellent survey method providing standardized and comparable information on wildlife density and abundance, particularly important for threatened species. Because of its highly diverse vertebrate community, SNP block South represents an excellent test-field, showing CTDS applicability to one of the remotest and least known rainforest areas of the globe. Density values

for the Congo peafowl, the giant ground pangolin, and the cusimanse presented here, are the first ever obtained, and are of critical conservation importance providing the basis for IUCN Red Lists species assessments. Despite limitations in comparability due to methodological differences and a site-specific ecological set-up, eight out of 11 densities obtained fell within published ranges (see Table S5). However, our estimates' accuracy remains to be confirmed: longitudinal assessments of density using standardized methods such as those detailed here will validate our results and shed light on the status of these cryptic species. Continuous monitoring and population trend evaluation are crucial information for wildlife conservation. Allowing simultaneous surveys of large portions of the terrestrial vertebrate community, rather than single species, the information CTDS can provide is of pivotal importance for the development of conservation plans of multi-species' communities. It may allow to reveal the delicacy of location specific ecological equilibria, crucial for the conservation of the integrity of the few remnant intact habitats of our planet.

ACKNOWLEDGEMENTS

This work was funded by Liverpool John Moores University and by the Kreditanstalt für Wiederaufbau (KfW Group) on behalf of the German Government and WWF Germany. We are grateful to all people that assisted data collection: R. Souza, M. Bofeko, R. Booto, B. Katembo, J. Kukumanga, S. Mwanduku, P. Musenzi, R. Ratsina, P. Bondo, G. Mbambe, W. Bokungu, P. Bokembi, E. Way, P. Ingange, J. Iyondo, B. Nkoy, A. Bomondjo. We thank S. Abedi, J. Eriksson, M. Etike, A. Kabamba, G. Kasiala, R. Keller, L. Lokumu, E. Lopongo, A. Louat, S. Matungila, M. Mbende, O. Nelson, for facilitating fieldwork; S. Mbongo, I. Di Dato, G. Kayembe, C. Kabamba, L. Nsenga, M. and T. de Sousa, for logistic support. We are grateful to the comments of S. Buckland, S. Focardi, E. Howe, F. Maisels, F. Michalski, L. Thomas and an anonymous reviewer. Special thanks go to B. Grothe, C. Röntrop, U. Zendel, A. Werner, R. McElreath, M. Tomasello, K. George, N. Jones, R. Leatherbarrow, A. Tattersall, and P. Wheeler. In DRC, we thank the *Institut Congolais pour la Conservation de la Nature*, the *Ministère de la Recherche Scientifique* and the *Unité de Gestion du Parc National de la Salonga*, for permitting research in Salonga National Park.

AUTHORS' CONTRIBUTIONS

H.S.K., G.H., I.H., K.P.N. and B.F. conceived the study; M.B., H.S.K., G.H., K.P.N., V.D. and B.F. organized data collection; P.A., P.B.D.C., E.D.B.F., B.I.B., M.D.I., M.A.K., D.B.M. and M.L.K.W. collected the data; I.B.I., P.K., G.H. and B.F. provided facilities and logistical support; M.B. and G.H. processed and analysed video footage; M.B. and B.F. wrote the manuscript with contributions from all co-authors.

DATA AVAILABILITY STATEMENT

Data available via the LJMU Data Repository <https://doi.org/10.24377/LJMU.d.00000052> (Bessone et al., 2020).

ORCID

Mattia Bessone  <https://orcid.org/0000-0002-8066-6413>

Barbara Fruth  <https://orcid.org/0000-0001-9217-3053>

REFERENCES

- Bahaa-el-din, L., Sollmann, R., Hunter, L. T., Slotow, R., Macdonald, D. W., & Henschel, P. (2016). Effects of human land-use on Africa's only forest-dependent felid: The African golden cat *Caracal aurata*. *Biological Conservation*, 199, 1–9. <https://doi.org/10.1016/j.biocon.2016.04.013>
- Bessone, M., Bondjengo, N., Hausmann, A., Herbing, I., Hohmann, G., Kuehl, H., ... Fruth, B. (2019). *Inventaire de la biodiversité dans le bloc sud du parc national de la Salonga et développement d'une stratégie de suivi écologique pour améliorer la protection de la faune et de la flore menacées dans le parc*. Final report. Berlin, Germany: ICCN-WWF-MPI-LMU.
- Bessone, M., Kühl, H. S., Hohmann, G., Herbing, I., N'Goran, K. P., Asanzi, P., ... Fruth, B. (2020). Data from: Drawn out of shadows: Surveying secretive forest species with camera trap distance sampling. *LJMU Data Repository*, <https://doi.org/10.24377/LJMU.d.00000052>
- Buckland, S. T., Anderson, D. R., Burnham, K. P., Laake, J. L., Borchers, D. L., & Thomas, L. (2001). *Introduction to distance sampling estimating abundance of biological populations*. Oxford, UK: Oxford University Press.
- Buckland, S. T., Rexstad, E. A., Marques, T. A., & Oedekoven, C. S. (2015). *Distance sampling: Methods and applications*. New York, NY: Springer.
- Burton, A. C., Neilson, E., Moreira, D., Ladle, A., Steenweg, R., Fisher, J. T., ... Boutin, S. (2015). Wildlife camera trapping: A review and recommendations for linking surveys to ecological processes. *Journal of Applied Ecology*, 52, 675–685. <https://doi.org/10.1111/1365-2664.12432>
- Campbell, D. (2005). *The Congo River basin. The world's largest wetlands: Ecology and conservation*. Cambridge, UK.
- Campos-Candela, A., Palmer, M., Balle, S., & Alós, J. (2017). A camera-based method for estimating absolute density in animals displaying home range behaviour. *Journal of Animal Ecology*, 87, 825–837. <https://doi.org/10.1111/1365-2656.12787>
- Cappelle, N., Després-Einspenner, M. L., Howe, E. J., Boesch, C., & Kühl, H. S. (2019). Validating camera trap distance sampling for chimpanzees. *American Journal of Primatology*, 81, e22962. <https://doi.org/10.1002/ajp.22962>
- Chandler, R. B., & Royle, J. A. (2013). Spatially explicit models for inference about density in unmarked or partially marked populations. *The Annals of Applied Statistics*, 7, 936–954. <https://doi.org/10.1214/12-AOAS610>
- Chauvenet, A. L., Gill, R. M., Smith, G. C., Ward, A. I., & Massei, G. (2017). Quantifying the bias in density estimated from distance sampling and camera trapping of unmarked individuals. *Ecological Modelling*, 350, 79–86. <https://doi.org/10.1016/j.ecolmodel.2017.02.007>
- Efford, M. G., Borchers, D. L., & Byrom, A. E. (2009). *Density estimation by spatially explicit capture-recapture: Likelihood-based methods. Modelling demographic processes in marked populations* (pp. 255–269). Boston, MA: Springer.
- Evans, M. J., & Rittenhouse, T. A. (2018). Evaluating spatially explicit density estimates of unmarked wildlife detected by remote cameras. *Journal of Applied Ecology*, 55, 2565–2574. <https://doi.org/10.1111/1365-2664.13194>
- Foster, R. J., & Harnsen, B. J. (2012). A critique of density estimation from camera-trap data. *The Journal of Wildlife Management*, 76, 224–236. <https://doi.org/10.1002/jwmg.275>
- Howe, E. J., Buckland, S. T., Després-Einspenner, M. L., & Kühl, H. S. (2017). Distance sampling with camera traps. *Methods in Ecology and Evolution*, 8, 1558–1565. <https://doi.org/10.1111/2041-210X.12790>
- Howe, E. J., Buckland, S. T., Després-Einspenner, M. L., & Kühl, H. S. (2019). Model selection with overdispersed distance sampling data. *Methods in Ecology and Evolution*, 10, 38–47. <https://doi.org/10.1111/2041-210X.13082>
- Hutchinson, J. M., & Waser, P. M. (2007). Use, misuse and extensions of "ideal gas" models of animal encounter. *Biological Reviews*, 82, 335–359. <https://doi.org/10.1111/j.1469-185X.2007.00014.x>

- IUCN. (2019). *The IUCN red list of threatened species*. Version 2019-1. Retrieved from <https://www.iucnredlist.org>
- Jackson, R. M., Roe, J. D., Wangchuk, R., & Hunter, D. O. (2006). Estimating snow leopard population abundance using photography and capture-recapture techniques. *Wildlife Society Bulletin*, 34, 772–781. [https://doi.org/10.2193/0091-7648\(2006\)34\[772:ESLPAU\]2.0.CO;2](https://doi.org/10.2193/0091-7648(2006)34[772:ESLPAU]2.0.CO;2)
- Kalan, A. K., Hohmann, G., Arandjelovic, M., Boesch, C., McCarthy, M. S., Agbor, A., ... Kühl, H. S. (2019). Novelty response of wild African apes to camera traps. *Current Biology*, 29, 1211–1217. <https://doi.org/10.1016/j.cub.2019.02.024>
- Karanth, K. U. (1995). Estimating tiger *Panthera tigris* populations from camera trap data using capture–recapture models. *Biological Conservation*, 71, 333–338. [https://doi.org/10.1016/0006-3207\(94\)00057-W](https://doi.org/10.1016/0006-3207(94)00057-W)
- Karanth, K. U., & Nichols, J. D. (1998). Estimation of tiger densities in India using photographic captures and recaptures. *Ecology*, 79, 2852–2862. [https://doi.org/10.1890/0012-9658\(1998\)079\[2852:EOTDII\]2.0.CO;2](https://doi.org/10.1890/0012-9658(1998)079[2852:EOTDII]2.0.CO;2)
- Kely, M. R., Kouakou, C. Y., Bene, J.-C.-K., Koffi, A. D., & N'guessan, K. A. & Tiedoue, M. R. (2019). Spatial distribution and period of activity of the forest elephant (*Loxodonta africana cyclotis*) at Taï National Park, south western Côte d'Ivoire. *Journal of Applied Biosciences*, 133, 13542–13551. <https://doi.org/10.4314/jab.v13.311.6>
- Kingdon, J., Happold, D., Butynski, T., Hoffmann, M., Happold, M., & Kalina, J. (2013). *Mammals of Africa*. London, UK: A&C Black.
- Linden, D. W., Sirén, A. P., & Pekins, P. J. (2018). Integrating telemetry data into spatial capture–recapture modifies inferences on multi-scale resource selection. *Ecosphere*, 9, e02203. <https://doi.org/10.1002/ecs2.2203>
- McGowan, P. J. K., Kirwan, G. M., & Sharpe, C. J. (2019). Congo Peafowl (*Afropavo congensis*). *Handbook of the birds of the world alive*. Barcelona, Spain: Lynx Edicions.
- Moeller, A. K., Lukacs, P. M., & Horne, J. S. (2018). Three novel methods to estimate abundance of unmarked animals using remote cameras. *Ecosphere*, 9, e02331. <https://doi.org/10.1002/ecs2.2331>
- Nakashima, Y., Fukasawa, K., & Samejima, H. (2017). Estimating animal density without individual recognition using information derivable exclusively from camera traps. *Journal of Applied Ecology*, 55, 735–744. <https://doi.org/10.1111/1365-2664.13059>
- Nichols, J. D., & Williams, B. K. (2006). Monitoring for conservation. *Trends in Ecology & Evolution*, 21, 668–673. <https://doi.org/10.1016/j.tree.2006.08.007>
- R Core Team. (2019). *R: A language and environment for statistical computing*. Vienna, Austria: R Foundation for Statistical Computing. Retrieved from <https://www.R-project.org/>
- Rich, L. N., Kelly, M. J., Sollmann, R., Noss, A. J., Maffei, L., Arispe, R. L., ... Di Bitetti, M. S. (2014). Comparing capture–recapture, mark-resight, and spatial mark-resight models for estimating puma densities via camera traps. *Journal of Mammalogy*, 95, 382–391. <https://doi.org/10.1644/13-MAMM-A-126>
- Rovero, F., & Zimmermann, F. (2016). *Camera trapping for wildlife research*. Exeter, UK: Pelagic Publishing Ltd.
- Rowcliffe, J. M., Carbone, C., Jansen, P. A., Kays, R., & Kranstauber, B. (2011). Quantifying the sensitivity of camera traps: An adapted distance sampling approach. *Methods in Ecology and Evolution*, 2, 464–476. <https://doi.org/10.1111/j.2041-210X.2011.00094.x>
- Rowcliffe, J. M., Field, J., Turvey, S. T., & Carbone, C. (2008). Estimating animal density using camera traps without the need for individual recognition. *Journal of Applied Ecology*, 45, 1228–1236. <https://doi.org/10.1111/j.1365-2664.2008.01473.x>
- Rowcliffe, J. M., Kays, R., Kranstauber, B., Carbone, C., & Jansen, P. A. (2014). Quantifying levels of animal activity using camera trap data. *Methods in Ecology and Evolution*, 5, 1170–1179. <https://doi.org/10.1111/2041-210X.12278>
- Smith, F. A., Lyons, S. K., Ernest, S. K. M., Jones, K. E., Kaufman, D. M., Dayan, T., ... Haskell, J. P. (2003). Body mass of Late Quaternary mammals. *Ecology*, 84, 3403–3403. <https://doi.org/10.1890/02-9003>
- Sollmann, R., Linkie, M., Haidir, I. A., & Macdonald, D. W. (2014). Bringing clarity to the clouded leopard *Neofelis diardi*: First density estimates from Sumatra. *Oryx*, 48, 536–539. <https://doi.org/10.1017/S0030.60531400043X>
- Sollmann, R., Mohamed, A., & Kelly, M. J. (2013). Camera trapping for the study and conservation of tropical carnivores. *Raffles Bulletin of Zoology*, 28, 21–42.
- Thomas, L., Buckland, S. T., Rexstad, E. A., Laake, J. L., Strindberg, S., Hedley, S. L., ... Burnham, K. P. (2010). Distance software: Design and analysis of distance sampling surveys for estimating population size. *Journal of Applied Ecology*, 47, 5–14. <https://doi.org/10.1111/j.1365-2664.2009.01737.x>
- Tobler, M. W., Carrillo-Percastegui, S. E., Pitman, R. L., Mares, R., & Powell, G. (2008). An evaluation of camera traps for inventorying large- and medium-sized terrestrial rainforest mammals. *Animal Conservation*, 11, 169–178. <https://doi.org/10.1111/j.1469-1795.2008.00169.x>
- Treves, A., Mwima, P., Plumptre, A. J., & Isoke, S. (2010). Camera trapping forest-woodland wildlife of western Uganda reveals how gregariousness biases estimates of relative abundance and distribution. *Biological Conservation*, 143, 521–528. <https://doi.org/10.1016/j.biocon.2009.11.025>

SUPPORTING INFORMATION

Additional supporting information may be found online in the Supporting Information section.

How to cite this article: Bessone M, Kühl HS, Hohmann G, et al. Drawn out of the shadows: Surveying secretive forest species with camera trap distance sampling. *J Appl Ecol*. 2020;57:963–974. <https://doi.org/10.1111/1365-2664.13602>